CrossMark

Interdecadal modulation on the relationship between ENSO and typhoon activity during the late season in the western North Pacific

Haikun Zhao[1] · Chunzai Wang[2]

Abstract The present study identifies an interdecadal modulation of the Pacific decadal oscillation (PDO) on the relationship between El Niño-Southern oscillation (ENSO) and typhoon activity during the late season (October–December) in the western North Pacific. The PDO is uncorrelated with ENSO during the warm phase of 1979–1997, while the PDO is positively correlated with ENSO during the cold phase of 1998–2012. Further analyses show that the warm phase is associated with the reduced ENSO–typhoon activity relationship and more typhoons, whereas the cold phase is corresponded to the enhanced ENSO–typhoon activity relationship and fewer typhoons. These variations are mainly manifested by a significant difference of typhoon activity in the southeastern part of the western North Pacific. Moreover, the change of ENSO–typhoon relationship is largely due to changes in large-scale environmental conditions especially from low-level vorticity and vertical wind shear between the two phases, which are related to the changes in tropical Indo-Pacific sea surface temperature. The study implies that the phase of the PDO should be taken into account when ENSO is used as a predictor for predicting typhoon activity in the western North Pacific.

1 Introduction

Among all of the ocean basins, the western North Pacific (WNP) is the most active region for tropical cyclone (TC) activity (Chan 2005). The WNP basin experiences about 26 TCs each year, accounting for 33 % of global TCs. TCs with maximum sustained winds equal to or greater than 64 knots (1 knot ~ 0.514 m/s) are known as typhoons in the WNP. Typhoon is one of the most destructive natural disasters, resulting in loss of life and property damage (Zhang et al. 2009). Therefore, a better understanding of typhoon or TC activity and the associated mechanisms has a profound socio-economic impact and scientific significance.

El Niño-Southern Oscillation (ENSO) is the strongest signal of the interannual variation of the ocean–atmosphere system and has a significant effect on global climate and extreme weather events such as TC activity (e.g., Wang and Chan 2002; Lander 1994; Chan 2000; Wang and Picaut 2004; Zhao et al. 2010, 2011). As an important source of interdecadal climate variability in the North Pacific, the Pacific decadal oscillation (PDO) has an ENSO-like spatial pattern in the sea surface temperature (SST) distribution (Mantua et al. 1997; Zhang et al. 1997). Previous studies documented that WNP TC activity experiences a significant interannual (Wang and Chan 2002; Lander 1994; Chen et al. 1998) and decadal/interdecadal variability (Yumoto and Matsuura 2001; Matsuura et al. 2003; Liu and Chan 2008; Chan 2006, 2008; Wang et al. 2010). It is further suggested that these changes are closely associated with ENSO and the PDO, which are the dominant modes of global

✉ Chunzai Wang
Chunzai.Wang@noaa.gov

[1] Pacific Typhoon Research Center, Earth System Modelling Center, Nanjing International Academy of Meteorological Sciences, Key Laboratory of Meteorological Disaster of Ministry of Education, Nanjing University of Information Science and Technology, Nanjing, China

[2] NOAA/Atlantic Oceanographic and Meteorological Laboratory, 4301 Rickenbacker Causeway, Miami, FL 33149, USA

climate on interannual (McPhaden 2002) and decadal (Mantuna and Hare 2002) time scales, respectively. For instance, there is a southeastward displacement of the mean TC genesis location during El Niño years compared to La Niña years (Chen et al. 1998; Wang and Chan 2002; Chia and Ropelewski 2002; Camargo and Sobel 2005; Camargo et al. 2007; Wang et al. 2013). Such a southeastward shift leads to longer durations and thus more intense TCs because TCs have more time and distance over the warm pool region of the WNP (Wang and Chan 2002; Camargo and Sobel 2005; Wu and Wang 2008; Wang et al. 2013; Zhao et al. 2011, 2014a). In contrast to a significant difference in the TC formation location, no significant change in the TC frequency between El Niño and La Niña years has been found (Lander 1994; Wang and Chan 2002). On decadal/interdecadal time scales, Ho et al. (2004) examined the interdecadal variability of the summertime typhoon tracks in the WNP. By comparing two periods of 1951–1979 and 1980–2001, they found that in the latter period the typhoon occurrence decreased significantly over the East China Sea and the Philippine Sea, but increased significantly over the South China Sea. Chan (2008) found that the decadal variations of the frequency and tracks of Categories 4 and 5 typhoons during May–November in the WNP are mainly due to the variations in global oceanic and atmospheric conditions associated with ENSO and the PDO.

A significant reduction of TC activity in the WNP since the 1990s has been recently reported (Liu and Chan 2013; Maue 2011; Tu et al. 2009; Yokoi and Takayabu 2013; Hsu et al. 2014; Zhao et al. 2014b). Liu and Chan (2013) suggested that a significant decrease of TC activity during the TC season (May–November) over the period of 1998–2011 is attributed to the increase of vertical wind shear in the WNP. By dividing the data into four seasons, a more recent study further pointed out that the significant decrease mainly resulted from an abrupt decrease of typhoon activity during the late season from October to December (Hsu et al. 2014). Hsu et al. (2014) examined the changes in large-scale fields in the recent decade compared to other decades, showing that the substantial basin-wide decrease of the TC genesis is mainly caused by the unfavorable dynamical environment factors such as the atmospheric low-level vorticity, vertical velocity, and vertical wind shear.

Studies have also examined the effects of the PDO and ENSO on global climate (Lee et al. 2012; Goodrich 2007; Wang et al. 2008; Kim et al. 2013) and illustrated that the PDO can significantly modulate ENSO related teleconnections over the globe, including the Indian summer monsoon (Krishnan and Sugi 2003; Krishnamurthy and Krishnamurthy 2013), and the East Asian winter monsoon (Wang et al. 2008), TC activity (Maue 2011; Girishkumar et al. 2014) and winter rainfall in Hawaii (Chu and Chen 2005). When the PDO and ENSO are in phase (out of phase), the relationship between ENSO and the associated climate anomalies is enhanced (reduced). In some regions, the relationship between ENSO and climate variations is more active only during a particular phase of the PDO (Gershunov and Barnett 1998; Power et al. 1999; Lupo and Johston 2000; Wang et al. 2008; Kim et al. 2013; Chowdary et al. 2012). However, impacts of the interdecadal modulation of the PDO on the relationship between ENSO and TC activity in the WNP during the late season have received less attention. The present paper focuses on the PDO relationships with ENSO and typhoon activity during the warm and cold phases of the PDO. The purpose of the present paper is to investigate these relationships, and the corresponding changes of large-scale atmospheric and oceanic conditions. Such an investigation is necessary and useful for the improvement of our understanding of interannual and decadal changes of typhoon activity in the WNP.

The remainder of this paper is organized as follows. Section 2 describes the datasets and methodologies used in this paper. Interdecadal modulation of the PDO on the relationship between ENSO and typhoon activity is presented in Sect. 3. The associated large-scale atmospheric and oceanic patterns and possible mechanism are investigated in Sect. 4. Discussion and summary are given in Sect. 5.

2 Data and methodologies

2.1 TC data

Observed techniques for TC activity in the WNP experienced three main stages: US Air Force aircraft from 1944 and 1987, meteorological satellite since 1971, and the development of the Dvorak intensity technique in 1977 (Emanuel 2005; Song et al. 2010; Ren et al. 2011). The uncertainty in TC wind speed estimates between TC datasets has become an important issue in understanding possible influence of climate change on TC activity. This uncertainty is mainly due to the inconsistent estimate technique among agencies and different computation methods of maximum sustained wind speed (Emanuel 2005; Song et al. 2010; Wu and Zhao 2012). For example, JTWC (Joint Typhoon Warning Center) uses 1-min average wind speed, JMA (Japan Meteorology Agency) chooses 10-min average wind speed, and STI-CMA (Shanghai Typhoon Institute of China Meteorology Administration) adopts 2-min average wind speed. As a result, some studies show inconsistent or even contradictory findings (Song et al. 2010; Kamahori et al. 2006; Wu and Zhao 2012).

Recently, using the intensity model developed by Emanuel et al. (2006, 2008), Wu and Zhao (2012) dynamically derived the basin-wide TC intensity in the WNP based on

Table 1 List of El Niño, La Niña and neutral years during the warm and cold phases of the PDO

	PDO warm phase (1979–1997)	PDO cold phase (1998–2012)
El Niño	1982, 1986, 1987, 1991, 1994, 1997	2002, 2004, 2006, 2009
Neutral	1979, 1980, 1981, 1985, 1989, 1990, 1992, 1993, 1996	2001, 2003, 2005, 2008, 2012
La Niña	1983, 1984, 1988, 1995	1998, 1999, 2000, 2007, 2010, 2011

the JTWC, STI-CMA and JMA datasets. The dynamically-derived intensity records are compared to those from the three best track datasets. It is found that the TC intensity data from JTWC is more reliable than the other two best track datasets. Therefore, the TC data during the late season from the JTWC are used in this study. As suggested by Hsu et al. (2014), the large decrease of annual typhoon counts in the WNP is mainly caused by the significant reduction of typhoons during the late season. To further confirm our analyses, we also used the STI-CMA and JMA datasets. Consistent results for the relationship between late season typhoon activity and ENSO events during the warm and cold phases of the PDO are found. In this study, we mainly focus on results from the JTWC best track dataset.

Typhoon positions are counted for each $2.5° \times 2.5°$ grid box in the WNP domain (0°–30°N, 100°E–180°E). The first position of a TC at which it is intensified into a typhoon (maximum sustained winds equal to or above 64 knots) is considered as typhoon position in the counting. The term "typhoon activity" is used in the rest of this study, unless otherwise explicitly stated. The typhoon track density is calculated by counting the number of typhoons forming within and passing through each grid box in the WNP.

2.2 Selection of ENSO events and PDO phases

The Niño-3.4 SST anomalies from the Climate Prediction Center are used to stratify El Niño and La Niña years by the threshold of 0.5 °C (−0.5 °C). The years with the SST anomalies during the late season (October to December) larger (less) than 0.5 °C (−0.5 °C) are defined as El Niño (La Niña) years. The other years are classified as neutral years. The PDO index used in this study is obtained from the Joint Institute for the study of Atmosphere and Oceans (JIASO) at University of Washington, which can be downloaded from http://jisao.washington.edu/pdo/PDO.latest. The PDO is defined as the leading principal component of monthly SST anomalies in the North Pacific poleward of 20°N (Mantua et al. 1997). The Niño-3.4 and PDO indices during the late-season are averaged to represent the status of ENSO and the PDO during the late season in this study.

The PDO shows a warm phase during the 1978–1997 and a cold phase during 1998–2012, which had been documented by many studies (Shen et al. 2006; Wang et al. 2009a, b). Thus, as shown in Table 1, six El Niño years

(1982, 1986, 1987, 1991, 1994, and 1997) and four El Niño years (2002, 2004, 2006, and 2009) are selected during the warm and cool phases of the PDO, respectively. Similarly, four La Niña years (1983, 1984, 1988, and 1995) and six La Niña years (1998, 1999, 2000, 2007, 2010, and 2011) are chosen during the warm and cool phases, respectively. The neutral years are also listed in Table 1.

2.3 Atmospheric and SST data

To explore the associated possible mechanism, the atmospheric variables (i.e., relative humidity, wind field and vertical velocity) are taken from the National Centers for Environmental Prediction and National Center for Atmospheric Research (NCEP/NCAR) Reanalysis II dataset at a $2.5° \times 2.5°$ grid (Kanamitsu et al. 2002). The monthly dataset of the Extended Reconstruction SST (ERSST) is obtained from the Climatic Data Center of National Oceanic and Atmospheric Administration at a horizontal resolution $2° \times 2°$ grid (Smith et al. 2008).

2.4 Bayesian change point analysis and statistical significance

To detect the abrupt shift in the time series of the typhoon number in the WNP during the late season, a Bayesian change point analysis is used (Chu and Zhao 2004; Tu et al. 2009; Zhao et al. 2014b; Hsu et al. 2014). Briefly, the seasonal TC counts are considered as a discrete Poisson process. The Poisson intensity (λ) is the only parameter and is codified by a conjugate gamma distribution. That is, if the prior probability density for λ is a gamma distribution, then the likelihood function for λ has the similar mathematical form. A hierarchical approach involving three layers—data, parameter, and hypothesis—is formulated to determine the posterior probability of the shift in time. The Bayesian inference provides the probability estimate of the shifts, rather a deterministic estimate of the change point location. This is an advantage over the deterministic approach because uncertainty inherent in statistical inference is quantitatively expressed in the probability statement and probability is the mathematical language of uncertainty.

Tests of statistical significance are usually performed using a Student's t test, assuming that two random variables follow a Gaussian distribution. Because of the relative small sample size in our 34-year analysis, it is not

guaranteed that the samples are characterized by the Gaussian distributions. Thus, instead of using a Student's *t* test, the non-parametric Mann–Kendall test (Mann 1945; Kendall 1975) and the Wilcoxon–Mann–Whitney test (Wilcoxon 1945; Mann and Whitney 1947) are used for assessing the significance of correlations and the difference between the two epochs (Chu 2002).

3 PDO modulation on the relationship between ENSO and typhoon activity

A recent reduction of the TC number in the WNP and of global TC activity was documented by Liu and Chan (2013) and Maue (2011), respectively. The time series of the TC and typhoon numbers in the WNP during the entire season (January to December) and the late season are shown in Figs. 1 and 2. We focus on the observed TC data after 1979 with satellite measurements. A common feature of these time series is the decrease of the TC and typhoon numbers around 1998. However, a significant and abrupt drop is observed in the TC or typhoon number during the late season (see Figs. 1, 2a). In this paper, we investigate and focus on typhoon variability during the late season.

The time series of the PDO index and the Nino3.4 index during the late season are shown in Fig. 3. The variations of these two indices are different during two periods of 1979–1997 and 1998–2012. Additionally, the separation of the two epochs is also based on the following reasons. First, the PDO transits into a cold phase after 1998. That is, the PDO is in a warm phase in the first epoch and a cold PDO phase in the second epoch, which was also documented in other studies (Shen et al. 2006; Wang et al. 2009a, b). Second, the Bayesian change-point analysis (see Sect. 2) of the typhoon frequency during the late season shows a great likelihood of a change point on the typhoon number in 1998 (Fig. 2b). This suggests a significant abrupt change of the typhoon number occurring in 1998. In fact, the average typhoon rate is 6.1 per year during the first epoch of 1979–1997 and dropped to 3.6 typhoons per year during the second epoch of 1998–2012.

The abrupt shift of the typhoon number during the late-season occurs in 1998, which is different from 1995 in Hsu et al. (2014). This difference is caused by using the different TC datasets. The JMA dataset was used in Hsu et al. (2014), while the JTWC dataset is used in this study. Moreover, the selection of typhoon cases in Hsu et al. (2014) is not based on the common definition of typhoons with sustained wind speed of over 64-kt. Simiu and Scanlon (1978) suggested that the strength of the 10-min sustained wind is statistically 88 % of the 1-min sustained wind. Therefore, Hsu et al. (2014) reduced the threshold from 64- to 56-kt 10-min wind speed for selecting typhoons in the JMA
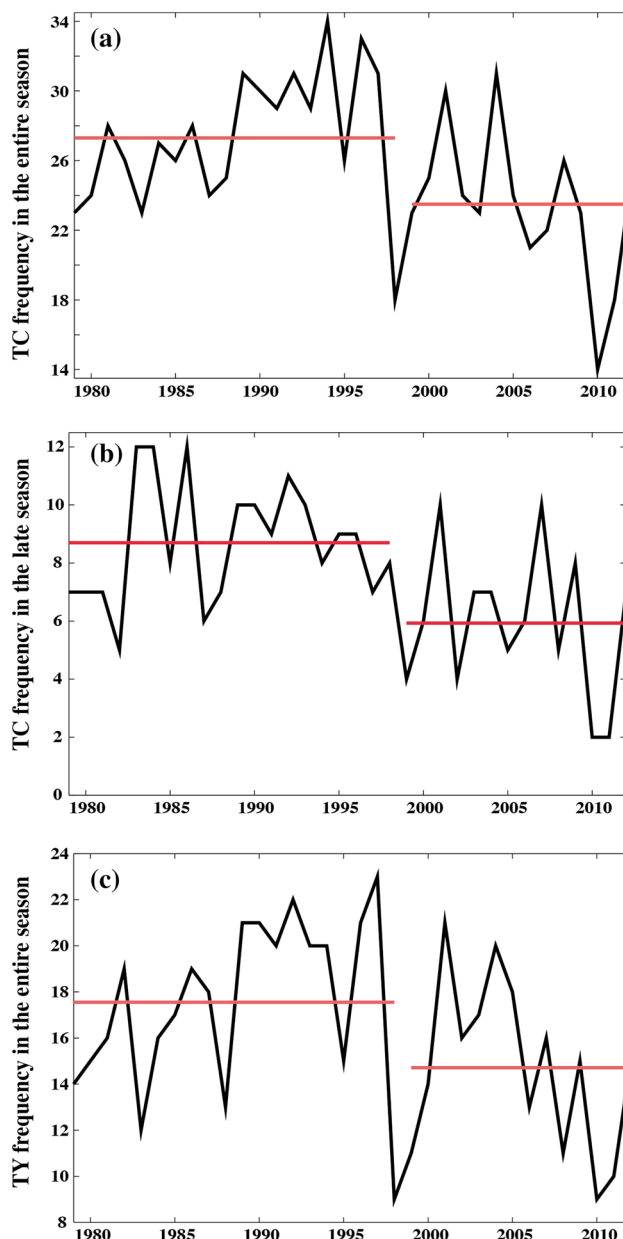

Fig. 1 Time series of **a** the TC number in the entire season (January to December), **b** the TC number in the late season (October to December), and **c** the typhoon number in the entire season. The *horizontal lines* represent the mean numbers during the warm phase of 1979–1997 and the cold phase of 1998–2012

dataset. Because of this conversion, the typhoon strength in Hsu et al. (2014) is weaker than that from the JMA official definition, which is based on a threshold of 64-kt 10-min sustained wind speed. Using the same change-point analysis method, we found that the typhoon numbers in peak and early seasons have no significant abrupt point, while only a significant abrupt point can be detected for the late season typhoon frequency (not shown). Additionally, we also computed the correlation between the Nino-3.4 index and

Fig. 2 a Time series of the typhoon number in the late season (October–December). **b** The conditional posterior probability mass function of change-points as a function of time. The *horizontal lines* in **a** represent the mean typhoon numbers during the warm phase of 1979–1997 and the cold phase of 1998–2012. See the text for the detail of calculating the conditional posterior probability mass function of change-points
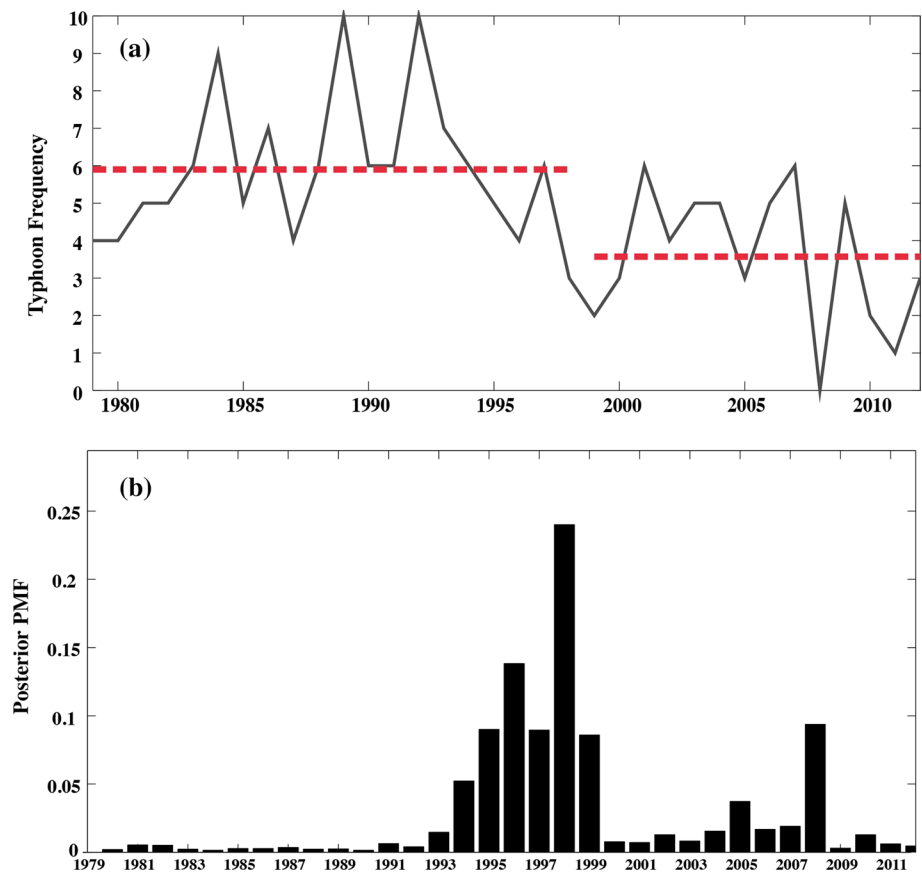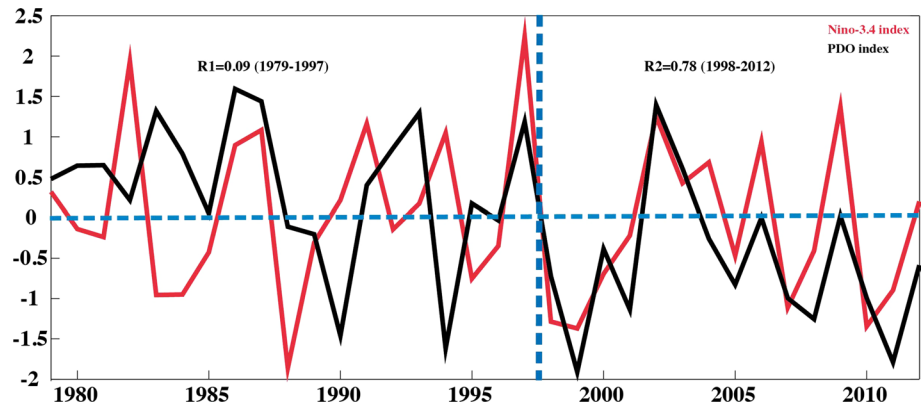
Fig. 3 Time series of PDO index (*black line*) and Niño3.4 index (*red line*) in the late season (October–December). The correlation of the PDO and Niño 3.4 index is 0.09 during the warm phase of 1979–1997 and is 0.78 during the cold phase of 1998–2012

PDO index averaged during January–March, April–June, and July–September. The results also show that the changing relationship between the PDO and ENSO for the peak and early seasons before and after 1998 is not so significant compared to the late season.

As shown in Fig. 3, a significant difference of correlations during the late season between the PDO and ENSO can be found in these two epochs, indicating an interdecadal shift of the relationship between the PDO and ENSO. During the warm phase of 1979–1997, the PDO and ENSO almost have no simultaneous correlation with a correlation

of 0.09, whereas a significant positive correlation with a correlation of 0.78 can be found during the cold phase of 1998–2012. Therefore, the relationship between the PDO and ENSO is not stationary over the past several decades, changing from a weak or no association to a stronger one after 1998. In other words, the PDO and ENSO are in phase during the cold phase of the PDO, and are uncorrelated during the warm phase of the PDO.

In the WNP, 168 typhoons occurred in the late season during 1979–2012. The climatological typhoon number is 4.94 each year with a standard deviation of 2.2, indicating
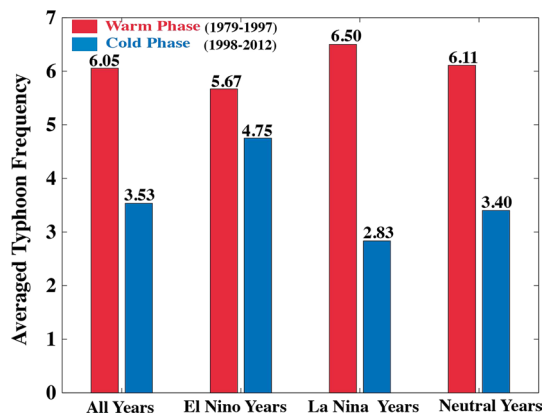
Fig. 4 Mean typhoon number for all years, El Niño years, La Niña years and neutral years during the warm phase of 1979–1997 and the cold Phase of 1998–2012. The typhoon differences between the warm and cold phases are statistically significant at the 95 % confidence level for all years, La Niña years and neutral years, but not for El Niño years. During the cold phase, the typhoon difference between El Niño years and La Niña years is statistically significant at the 95 % confidence level. During the warm phase, no significant differences are found

a strong interannual variation of the typhoon number in the late season. As shown in Fig. 4, more typhoons (6.05 typhoons) can be found during the warm phase compared to those during the cold phase (3.53 typhoons). The difference between the warm and cold phases is 2.45 and larger than 1 standard deviation, which is significant above the 95 % confidence level. Furthermore, it is shown that the significant difference of typhoons between the warm and cold phases is mainly due to significant differences during La Niña and neutral years. For La Niña years, 6.50 typhoons occur during the warm phase and 2.83 typhoons appear during the cold phase; their difference is significant above the 95 % confidence level. For neutral years, the difference in typhoon counts between the warm and cold phase is also statistically significant above the 95 % confidence

level (6.11 vs. 3.40). For El Niño years, 5.67 typhoons are observed during the warm phase, which is insignificantly higher than 4.75 during the cold phase.

During the warm phase, there is a tendency for more typhoons to form in La Niña (6.50) and neutral years (6.11) than that in El Niño years (5.67), but the difference is not significant. This indicates that there is no ENSO–typhoon number relationship during the warm phase. However, the cold phase shows significant more typhoons (4.75) in El Niño years compared to in La Niña years (2.83). Meanwhile, slightly more typhoons occur in neutral years than those in La Niña years during the cold phase. In comparison with the warm phase, the cold phase shows an enhanced relationship between ENSO and the typhoon number. In other words, there is no relationship between ENSO and typhoons in the late season during warm phase, whereas El Niño years show more typhoons than La Niña years during the cold phase.

For the formation location, a significant increase of typhoons can be found in the southeastern part of the WNP during the warm phase compared to that during the cold phase for El Niño years (Fig. 5a). Typhoons tend to follow a northwestward track with the typhoon track density distribution oriented from 5°N, 165°E to the east of Luzon during the warm phase compared to that during the cold phase (Fig. 5c). There is a substantial reduction between 20°N, 150°E and 5°N, 135°E and in the South China Sea when La Niña events occur during the cold phase (Fig. 5b). For La Niña years, although typhoons still tend to move mainly westward during the warm phase (Fig. 5d), the track is much shorter and is confined in the Philippine Sea relative to the corresponding one when El Niño events occur (Fig. 5c). Moreover, there is an indication that typhoons may recurve poleward near 135°E (Fig. 5d). More typhoons are observed over the South China Sea when La Niña events occur during the cold phase.

Fig. 5 Composite differences of typhoon genesis distribution (×100) between the cold and warm phases for **a** El Niño years and **b** La Niña years. The corresponding **c** and **d** are the differences of typhoon track density distribution (×10). *Shading* indicates that the difference is statistically significant at the 95 % confidence level
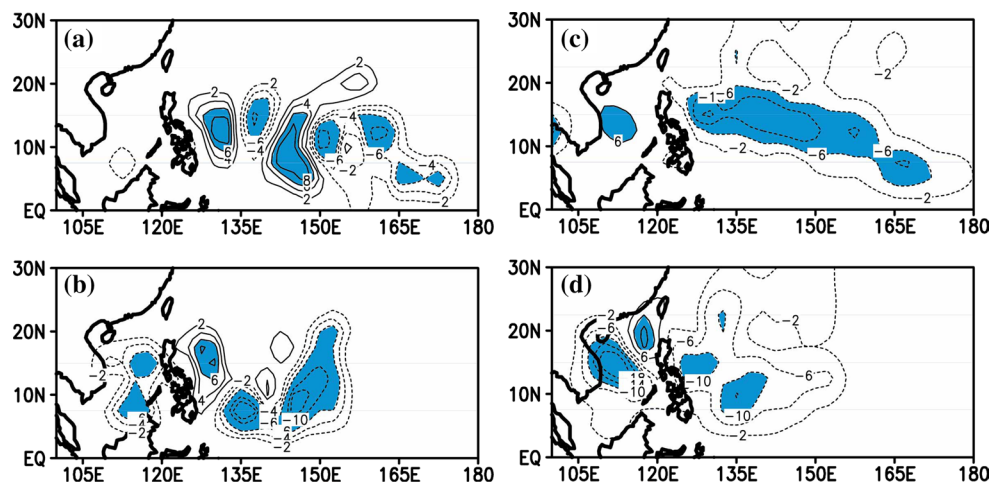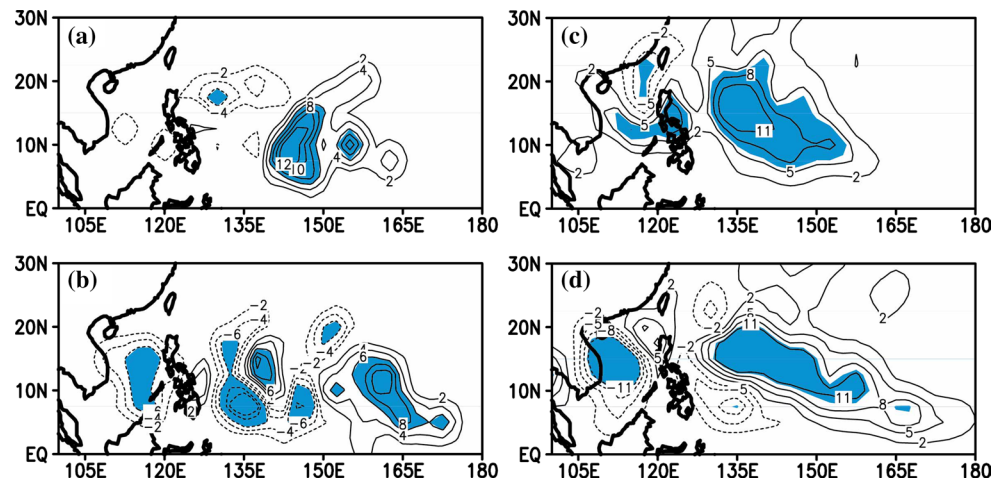
Fig. 6 Composite differences of **a** typhoon genesis distribution (×100) and **c** typhoon track density distribution (×10) between El Niño years and La Niña years during the cold phase. The corresponding **b** and **d** are the differences during the warm phase. *Shading* indicates that the difference is statistically significant at the 95 % confidence level

During the cold phase of the PDO (Fig. 6a), an east–west dipole of the genesis location is shown over the tropical WNP, with a major positive center in the area from 140°E to 150°E and a negative one to the east of Philippines, suggesting a southeastward shift in the typhoon formation location from La Niña to El Niño years. The typhoon track density distribution during the cold phase is also featured by a zonal dipole pattern (Fig. 6c). Larger typhoon track density prevails from the west of 165°E extending westward across Philippines to the central South China Sea when El Niño occurs relative to La Niña. On the other hand, fewer (more) typhoon occurrences are observed along the coast of southeast China and Taiwan during El Niño (La Niña) events (Fig. 6c). During the warm phase, the major region of the genesis location is shifted even more eastward compared to that during the cold phase (Fig. 6a, b). As a result, the typhoon track becomes elongated in a southeast to northwest orientation from 5°N, 170°E to approximately 20°N, 125°E when El Niño events occur (Fig. 6d). In comparison with the cold phase, the warm phase shifts the major genesis location eastward when El Niño events occur. That is, more typhoons are expected to occur to the east of 155°E in the tropical WNP when El Niño occurs during the warm phase of the PDO, and a higher frequency of typhoon is formed to the west of 150°E when El Niño occurs during the cold phase of the PDO.

In summary, the interdecadal modulation of the PDO can change the relationship between ENSO and typhoon activity during the late season. During the warm phase of the PDO, the PDO is uncorrelated with ENSO; the relationship between ENSO and the typhoon number is reduced; and more typhoons occur. During the cold phase of the PDO, the PDO is positively correlated with ENSO; the relationship between ENSO and the typhoon number is enhanced; and fewer typhoons are observed. Moreover, it is

interesting that a consistent result—with the southeastward shift of the formation location and more typhoons with the northwestward tracks during the warm phase compared to the cold phase for all ENSO events—is observed. In the following sections, we attempt to explore the plausible physical reasons for these associated differences of ENSO–typhoon activity during the late season in the WNP.

4 The associated large-scale patterns and possible explanation

The TC genesis is generally dominated by favorable environmental conditions. An increase of the low-level cyclonic vorticity is favorable for the TC development of convection and intensification by reducing the local Rossby radius of deformation and then focusing the convective heating locally (Chen et al. 2006). The presence of significant vertical wind shear inhibits the TC development by advecting the heating and moisture away from the convention center (DeMaria 1996). In this study, the vertical wind shear is computed as the difference of wind vectors between 200 and 850 hPa:

$$V_{shear} = \sqrt{(u_{200} - u_{850})^2 + (u_{850} - u_{850})^2}$$

The higher mid-level humidity makes a parcel of air be able to remain saturated as it entrains the surrounding air during its ascent and is conductive for maintaining convective activity of the TC development (Kaplan et al. 2010; Li et al. 2013). In the following sections, the environmental conditions associated with the TC genesis will be examined based upon the composite analysis to understand the possible physical reasons of changes in the relationship between ENSO and typhoon activity during the late season in the WNP.

Fig. 7 Composite differences of **a** 850 hPa wind and relative vorticity ($\times 10^6$) and **c** vertical wind shear between El Niño years and La Niña years during the cold phase. The corresponding **b** and **d** are the differences during the warm phase. *Shading* indicates that the difference is statistically significant at the 95 % confidence level
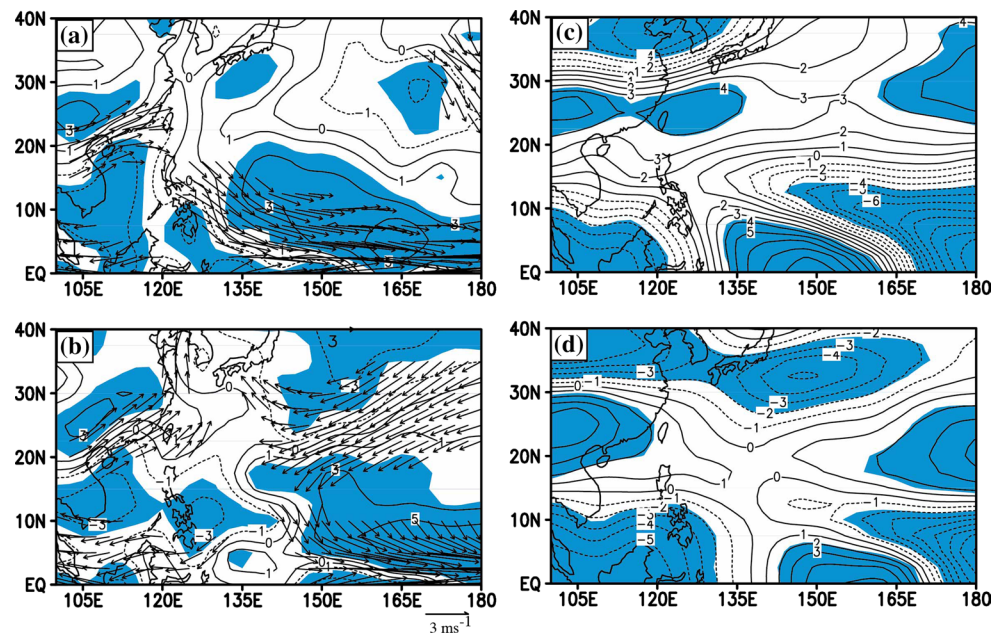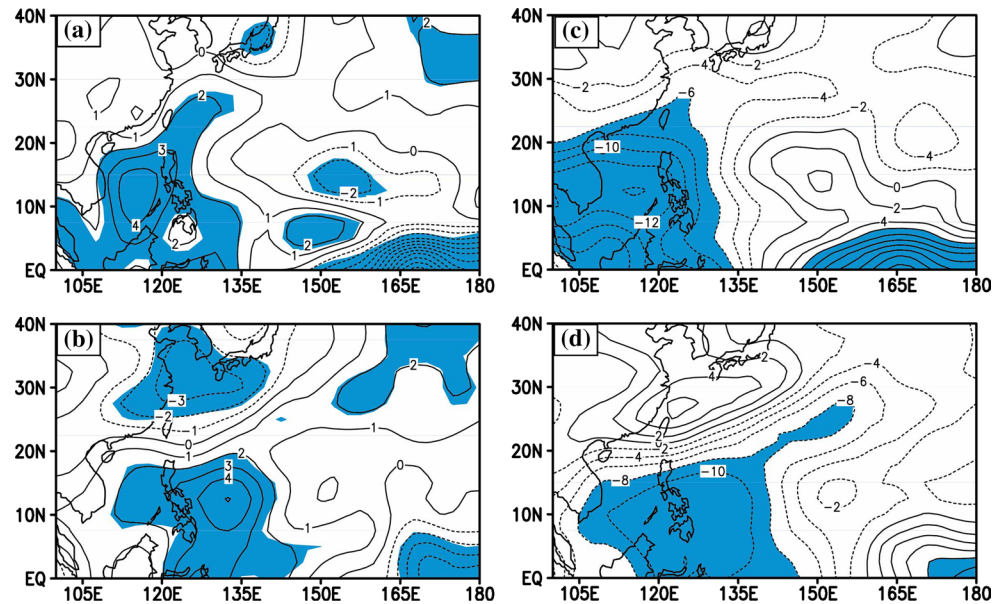

Fig. 8 Composite differences of **a** 500 hPa omega ($\times 100$) and **c** 600 hPa relative humidity ($\times 10$) between El Niño year and La Niña years during the cold phase. The corresponding **b** and **d** are the differences during the warm phase. *Shading* indicates that the difference is statistically significant at the 95 % confidence level

4.1 Changes in local large-scale atmospheric conditions

As shown in Fig. 7a, a significant enhancement of low-level vorticity and positive zonal wind anomalies in the southeastern part (135°E–180°, 0–17°N) of the WNP for El Niño years compared to those for La Niña years during the cold phase. These are consistent with more typhoons in the southeastern part of the WNP for El Niño years compared to La Niña years during the cold phase (Fig. 6a). Similar results can also be found during the warm phase, but a cyclonic circulation pattern occurs further eastward in the southeastern part from 150°E to dateline (Fig. 7b),

which is also corresponded to changes in the typhoon genesis location (Fig. 6b) between El Niño and La Niña years. The change of vertical wind shear displays a similar result (Fig. 7c, d) with the negative wind shear anomalies in the southeastern part of the WNP which favor typhoon activity there. The vertical velocity of 500-hPa omega and relative humidity are shown in Fig. 8. It is shown that the moderately decreased vertical velocity is located in a small region adjacent to the equatorial belt for El Niño years compared to that for La Niña years. Similar results can also found for increased relative humidity in the equatorial belt. In summary, the difference of the typhoon genesis associated with

Fig. 9 Composite differences of **a** 850 hPa wind and relative vorticity ($\times 10^6$) between the cold phase and the warm phase for **a** El Niño years and **b** La Niña years. The corresponding **c** and **d** are the *vertical* wind shear. *Shading* indicates that the difference is statistically significant at the 95 % confidence level
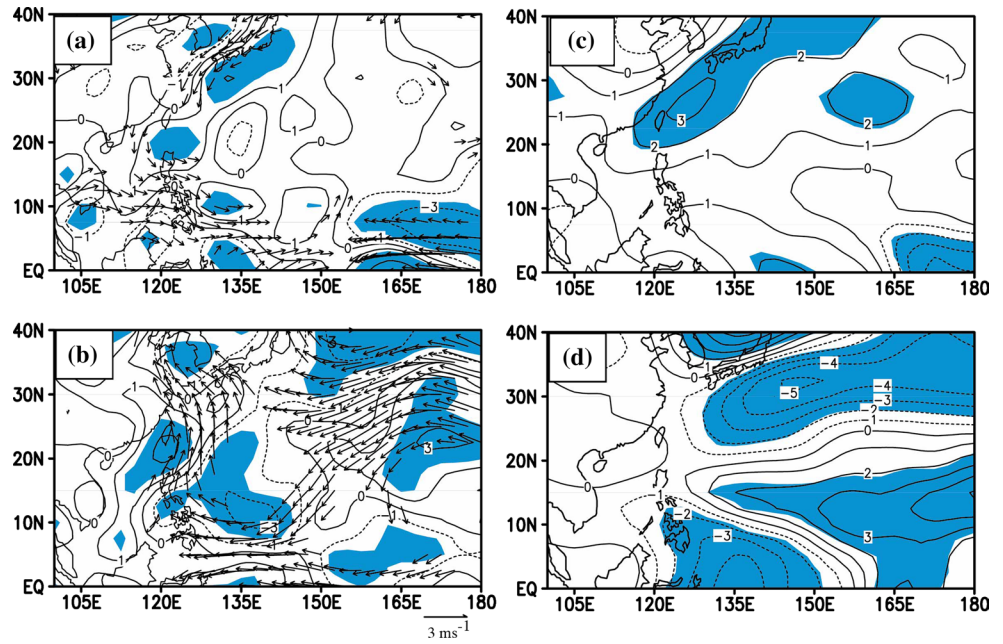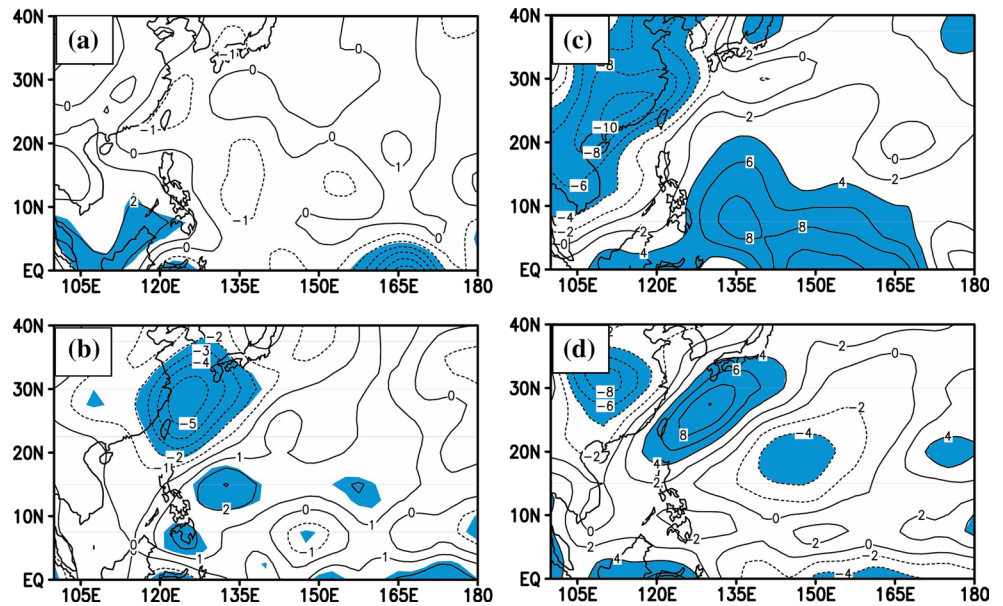

Fig. 10 Composite differences of 500 hPa omega ($\times 100$) between the cold phase and the warm phase for **a** El Niño years and **b** La Niña years. The corresponding **c** and **d** are 600 hPa relative humidity ($\times 10$). *Shading* indicates that the difference is statistically significant at the 95 % confidence level

ENSO during a specific phase (the cold or warm phase) is mainly due to the changes in the low-level relative vorticity and vertical wind shear although the vertical velocity and relative humidity also play some roles in the typhoon genesis.

Similar analysis is performed for the difference of associated large-scale atmospheric fields between the cold and warm phases for El Niño and La Niña years (Figs. 9, 10). It is seen that the low-level relative vorticity and vertical wind shear are also the most important dynamical factors to the change of typhoon activity for El Niño and La Niña years in the WNP between the two periods, particularly in

the southeastern part of the WNP. Compared to the warm phase, the cold phase shows significant negative low-level relative vorticity anomalies and decreased vertical wind shear over the southeastern part of the WNP for El Niño years. For La Niña years, a southeast-northwest region with negative low-level vorticity and significant enhanced vertical wind shear are found during the cold phase compared to the warm phase. These results are consistent with the changes of typhoon activity in the WNP in the late season during the cold phase. As shown in Fig. 10a, b, no significant difference of vertical velocity can be found for El Niño and La Niña years. In addition, compared to the warm
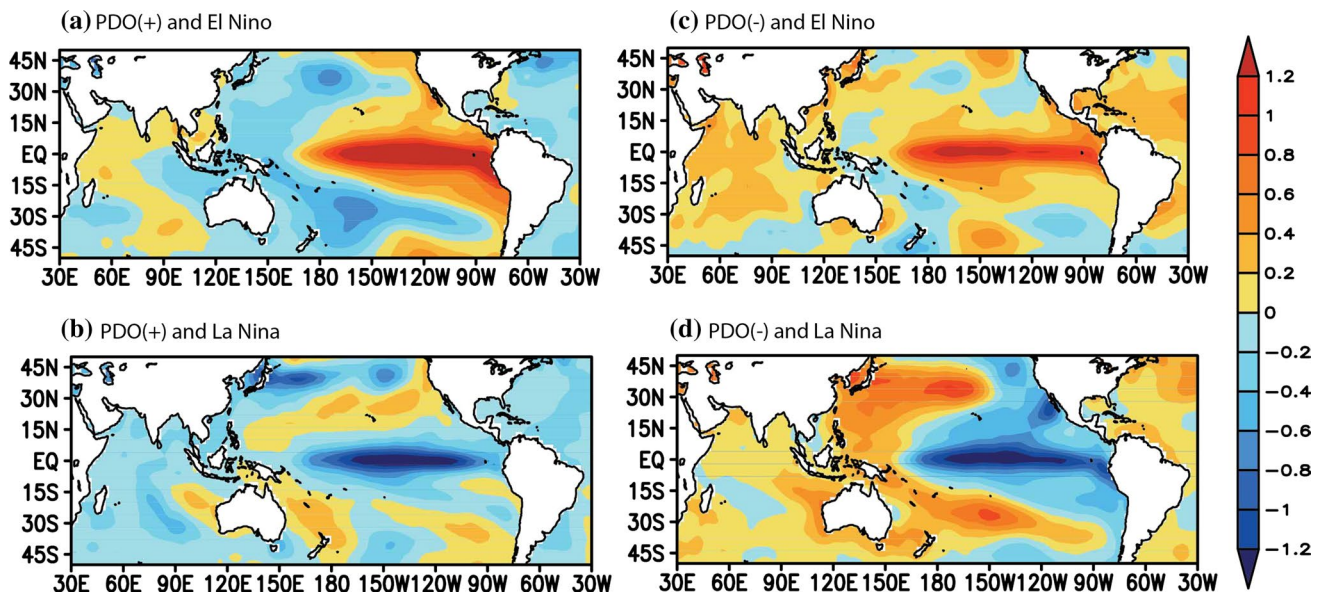
Fig. 11 Composites of SST anomalies during **a** the warm phase of the PDO and El Niño years, **b** the warm phase of the PDO and La Niña years, **c** the cold phase of the PDO and El Niño years, and **d** the cold phase of the PDO and La Niña years

phase, the cold phase shows the remarkable increase of relative humidity over the southeastern region of the WNP for El Niño years (Fig. 10c), which favors the TC genesis. For La Niña years, a small decrease of relative humidity over the southeastern region of the WNP (Fig. 10d). These suggest that the relative humidity plays a role in determining the large difference of the typhoon genesis in the southeastern region of the WNP.

4.2 Changes in SST anomalies

The composites of SST anomalies during the warm and cold phases of the PDO for El Niño and La Niña years are shown in Fig. 11. The composite of SST anomalies for El Niño years during the warm phase of 1979–1997 shows a warming in the western coast of South America (Fig. 11a), whereas the composite during the cold phase of 1998–2012 does not show the South American coast warming with the large warming in the equatorial central Pacific (Fig. 11c). This is because the recent cold phase of 1998–2012 is dominated by the Central Pacific (CP) El Niño events and the warm phase of 1979–1997 is largely associated with the Eastern Pacific (EP) El Niño events. More CP El Niño events during the recent decade have been documented and discussed in previous studies (Xiang et al. 2013; Zhang et al. 2014). These studies suggested that more CP warm events in the second epoch of 1998–2012 might be mainly affected by the abrupt climate change. The interdecadal shift of the relationship between the PDO and ENSO may also a cause. These are beyond our scope of this study and deserve for a further investigation.
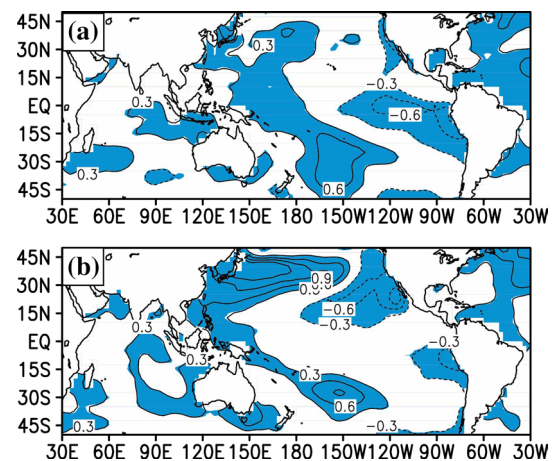

Fig. 12 Composite differences of SST anomalies between the cold phase and the warm phase for **a** El Niño years and **b** La Niña years. *Shading* indicates that the difference is statistically significant at the 95 % confidence level

The SST anomaly differences between the cold and warm phases show cooling in the eastern Pacific and warming in the western Pacific and Indian Oceans (Fig. 12). Additionally, the tropical oceans show a warmer tendency including the western Pacific and Indian Oceans for El Niño years during the cold phase relative to those during the warm phase (Fig. 12a). Similar SST anomaly difference between the cold and warm phases for La Niña years is also shown in Fig. 12b. Note that a difference of SST anomaly amplitude can be found for El Niño and La Niña years between the cold and warm phases. The SST anomalies
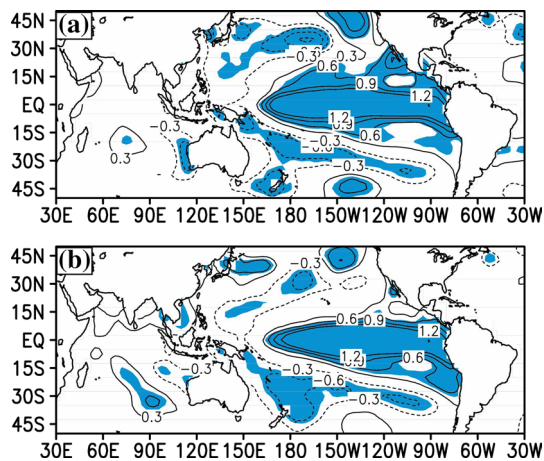
Fig. 13 Composite differences of SST anomalies between El Niño years and La Niña years during **a** the cold phase and **b** the warm phase. *Shading* indicates that the difference is statistically significant at the 95 % confidence level

show a significant difference in the eastern Pacific. A largest region with cool SST anomalies occurs in the equatorial eastern Pacific for El Niño years; the cooling is confined to the region close to the South American coast for La Niña years. Further, it is found that the SST anomaly patterns between El Niño and La Niña years during the cold and warm phases (Fig. 13) are similar, but the amplitude of SST anomalies shows somewhat difference.

4.3 Possible explanation

As suggested by previous studies (Zhan et al. 2011; Zhang et al. 2007; Zhao et al. 2014b; Hsu et al. 2014), the different SST anomaly distributions can impact different circulations in the WNP. The dramatic SST decadal changes in the Indo-Pacific region are warm SST anomalies that have been shown in previous studies (Burgman et al. 2008; Chikamoto et al. 2012; Wang et al. 2013; Hong et al. 2014; Hsu et al. 2014). As indicated by Chan (2008) and Hsu et al. (2014), the change of typhoons is unlikely to be controlled by thermodynamic factors. They found that warm SST anomalies in the tropical Indo-Pacific Ocean contribute negatively to the decrease in the typhoon genesis by inducing a significant change in low-level circulations in the southeastern region of the WNP. The linkage between the tropical Indo-Pacific SST and the southeastern atmospheric circulations of the WNP has been addressed in previous studies (Weisberg and Wang 1997; Wang et al. 1999, 2013, 2015; Hsu et al. 2014).

The warm SST anomalies in the tropical Indian Ocean can excite a warm equatorial Kelvin wave to the east in the troposphere (Xie et al. 2009; Zhan et al. 2011; Tao et al. 2012), enhancing the atmospheric anticyclonic anomaly

over the WNP that is forced by SST anomalies from El Nino events (Weisberg and Wang 1997; Wang et al. 1999). As shown in Figs. 11 and 12, the cold phase is associated with warm SST anomalies in the Indian Ocean which can cause anticyclonic circulation in the WNP. Meanwhile, warm SST anomalies in the western Pacific are observed during the cold phase compared to those during the warm phase, which will cause equatorial wind anomalies and thus change atmospheric circulations associated with the monsoon trough.

As illustrated by Hsu et al. (2014), the recent cooling in the eastern Pacific plays a secondary role in causing unfavorable conditions for the TC genesis in the southeastern part of the WNP. They found that the combined effect of warm SST in the WNP and Indian Ocean plays a key role in the typhoon decrease in the WNP by causing atmospheric circulation to the east of 140°E, which is responsible for the reduced typhoon counts. The Indian Ocean warming produces an anomalous anticyclone in the WNP, which is confined to the west of 140°E. Associated with these results and Figs. 11 and 12, it is suggested that a significant warm SST anomaly in the tropical WNP and Indian Ocean during the cold phase compared to that during the warm phase could cause atmospheric circulation anomalies in the WNP.

5 Discussion and summary

During 1979–2012, 7 typhoons occurred approximately each year during the late season in the WNP. Since the late-season typhoon activity has caused catastrophic damages to the Philippines and to other Asian countries in the recent years, it is important to study typhoon activity during the late season. Recently, Hsu et al. (2014) found an abrupt shift in the late season typhoon counts occurring in 1995 based upon the JMA best track dataset. Associated with the dominant interannual and decadal climate signals of ENSO and the PDO, studies have suggested that the combined the PDO and ENSO had a significant modulation of global climate (Wang et al. 2008). Previous studies focused on TC activity associated with either the PDO phases or ENSO events, but the PDO's modulation on the relationship between ENSO and typhoon activity has not been investigated.

Based upon the JTWC best track dataset from 1979 to 2012, we find that the interdecadal shift of relationship between the PDO and ENSO occurs in 1998. During 1979–1997, the PDO is not related to ENSO, while the PDO is positively correlated with ENSO during 1998–2012. The first epoch of 1979–1997 is during the warm phase of the PDO, while the second epoch of 1998–2012 is during the cold phase of the PDO. Associated with the interdecadal shift of the relationship between the PDO and ENSO, the

relationship between ENSO and typhoon activity during the late season in the WNP in the two epochs is investigated. The present study identifies a clear interdecadal modulation of the PDO on the relationship between ENSO and typhoon activity during the late season in the WNP.

A significant difference in the typhoon number between the two phases is observed: 6.05 typhoons per year during the warm phase and only 3.53 typhoons per year during the cold phase, which is mainly due to the large difference in La Niña and neutral years. During the warm phase, the typhoon frequency for El Niño, La Niña and neutral years shows a slight difference, but the typhoon genesis region shows a significant southeastward shift for El Niño years compared to that for La Niña years. Different from that during the warm phase, during the cold phase the typhoon frequency for El Niño years and La Niña years shows a significant difference. During the cold phase, 4.75 typhoons per year occurred for El Niño years, while 2.83 typhoons formed for La Niña years. Meanwhile, the TC genesis location also shows a significant southeastward shift for El Niña years compared to that for La Niña years. In summary, the reduced ENSO–typhoon activity relationship and more typhoons are detected during the warm phase, while the enhanced ENSO–typhoon activity relationship and fewer typhoons are observed during the cold phase.

Our analyses further indicate that the change of ENSO–typhoon relationship between the two phases is mainly due to changes in the environmental factors especially from the dynamical factors of low level vorticity and vertical wind shear. Compared to that during the cold phase, the warm phase shows the significant increase of cyclonic vorticity in the southeastern part of the WNP. These changes of environmental factors are mainly induced by changes in SST anomalies. Compared to the cold phase, a similar SST anomaly pattern during the warm phase for El Niño and La Niña years is found although the SST warming and cooling magnitude shows slight different. The SST anomaly distribution pattern is similar to that in Hsu et al. (2014). So we can speculate that the change in the relationship between ENSO and typhoon activity is mainly due to the changes in SST anomalies between the two phases. The Indian Ocean and western Pacific SST warming may play a significant role in the causing the atmospheric circulation changes in the WNP especially for La Niña years. The eastern/central Pacific warming plays a negligible impact on the southeastern part of the WNP. In addition, as shown in Fig. 11, the Atlantic SST anomalies are also warm, which may relate to the atmospheric circulation in the WNP (Ham et al. 2013; Zhang et al. 2014). The effects of the remote and local SST anomalies on the WNP circulation are worthy further investigation. Moreover, interdecadal modulation of ENSO amplitude and its influence on the WNP as shown in Chowdary et al. (2012) may also be important.

Finally, the interdecadal change of the relationship between the PDO and ENSO has an impact on the relationship between ENSO and typhoon activity during the late season. Currently, many studies attempt to predict the seasonal TC activity of the WNP using ENSO as a predictor (Chan 2005; Wang and Zhou 2008). According to our analyses in this study, the phase of the PDO should be taken into account when ENSO is used as a predictor for TC activity in the WNP. By doing so, it may provide us a better outlook or prediction of typhoon activity in the WNP.

References

Burgman RJ, Schopf PS, Kirtman BP (2008) Decadal modulation of ENSO in a hybrid coupled model. J Clim 21:5482–5500

Camargo SJ, Sobel AH (2005) Western North Pacific tropical cyclone intensity and ENSO. J Clim 18:2996–3006

Camargo SJ, Emanuel KA, Sobel AH (2007) Use of a genesis potential index to diagnose ENSO effects on tropical cyclone genesis. J Clim 20:4819–4834

Chan JCL (2000) Tropical cyclone activity over the western North Pacific associated with El Niño and La Niña events. J Clim 13:2960–2972

Chan JCL (2005) Interannual and interdecadal variations of tropical cyclone activity over the western North Pacific. Meteorol Atmos Phys 89:143–152

Chan JCL (2006) Comments on "Changes in tropical cyclone number, duration, and intensity in a warming environment". Science 311:1713

Chan JCL (2008) Decadal variations of intense typhoon occurrence in the western North Pacific. Proc R Soc Lond 464A:249–272

Chen T-C, Weng S-P, Yamazaki N, Kiehne S (1998) Interannual variation in the tropical cyclone formation over the western North Pacific. Mon Weather Rev 126:1080–1090

Chen GT, Wang C-C, Lin L-F (2006) A diagnostic study of a retreating Mei-Yu front and the accompanying low-level jet formation and intensification. Mon Weather Rev 134:874–896

Chia H-H, Ropelewski C-F (2002) The interannual variability in the genesis location of tropical cyclones in the northwest Pacific. J Clim 15:2934–2944

Chikamoto Y et al (2012) Predictability of a stepwise shift in Pacific climate during the late 1990s in hindcast experiments using MIROC. J Meteorol Soc Jpn 90A:1–21. doi:10.2151/jmsj.2012-A01

Chowdary JS, Xie SP, Tokinaga H, Okumura YM, Kubota H, Johnson N, Zheng XT (2012) Interdecadal variations in ENSO teleconnection to the Indo-Western Pacific for 1870–2007. J Clim 25:1722–1744

Chu PS (2002) Large-scale circulation features associated with decadal variations of tropical cyclone activity over the central North Pacific. J Clim 15:2678–2689

Chu PS, Chen H (2005) Interannual and interdecadal rainfall variations in the Hawaiian Islands. J Clim 18:4796–4813

Chu PS, Zhao X (2004) Bayesian change-point analysis of tropical cyclone activity: the Central North Pacific case. J Clim 17:4893–4901

DeMaria M (1996) The effect of vertical wind shear on tropical cyclone intensification change. J Atmos Sci 53:2076–2088

Emanuel KA (2005) Increasing destructiveness of tropical cyclones over the past 30 years. Nature 436:686–688

Emanuel KA, Ravela S, Vivant E, Risi C (2006) A statistical-deterministic approach to hurricane risk assessment. Bull Am Meteorol Soc 87:299–314

Emanuel K, Sundararajan R, Williams J (2008) Hurricanes and global warming: results from downscaling IPCC AR4 simulations. Bull Am Meteorol Soc 89:347–367

Gershunov A, Barnett TP (1998) Interdecadal modulation of ENSO teleconnections. Bull Am Meteorol Soc 79:2715–2725

Girishkumar MS, Prakash VT, Ravichandran M (2014) Influence of Pacific decadal oscillation on the relationship between ENSO and tropical cyclone activity in the Bay of Bengal during October–December. Clim Dyn 44(11–12):3469–3479

Goodrich GB (2007) Influence of the Pacific decadal oscillation on winter precipitation and drought during years of neutral ENSO in the western United States. Weather Forecast 22:116–124

Ham YG, Kug JS, Park JY, Jin FF (2013) Sea surface temperature in the north tropical Atlantic as a trigger for El Niño/Souther Oscillation events. Nat Geosci 6:112–116

Ho CH, Baik JJ, Kim JH, Gong DY, Sui CH (2004) Interdecadal changes in summertime typhoon tracks. J Clim 17(9):1767–1776

Hong C-C, Li T, Wu Y-K, Chang C-C (2014) The climate regime shift over the Pacific during 1996/1997. Clim Dyn 43(1–2):435–446

Hsu PC, Chu PS, Murakami H, Zhao X (2014) An abrupt decrease in the late-season typhoon activity over the western North Pacific. J Clim 27:4296–4312

Kamahori HN, Yamazaki N, Mannoji N, Takahashi K (2006) Variability in intense tropical cyclone days in the western North Pacific. SOLA 2:104–107. doi:10.2151/sola.2006-027

Kanamitsu M, Ebisuzaki W, Woolen J, Yang S-K, Hnilo JJ, Fiorino M, Potter GL (2002) NCEP-DOE AMIP-II reanalysis (R-2). Bull Am Meteorol Soc 83:1631–1643

Kaplan JM, DeMaria J, Knaff A (2010) A revised tropical cyclone rapid intensification index for the Atlantic and eastern North Pacific Basins. Weather Forecast 25:220–241

Kendall MG (1975) Rank correlation methods. Charles Griffin, 202 pp

Kim J-W, Yeh S-W, Chang E-C (2013) Combined effect of El Niño-Southern oscillation and Pacific decadal oscillation on the East Asian winter monsoon. Clim Dyn. doi:10.1007/s00382-013-1730-z

Krishnamurthy L, Krishnamurthy V (2013) Influence of PDO on South Asian summer monsoon and monsoon–ENSO relation. Clim Dyn 42:2397–2410

Krishnan R, Sugi M (2003) Pacific decadal oscillation and variability of the Indian summer monsoon rainfall. Clim Dyn 21:233–242

Lander MA (1994) An exploratory analysis of the relationship between tropical storm formation in the western North Pacific and ENSO. Mon Weather Rev 122:636–651

Lee HS, Yamashita T, Mishima T (2012) Multi-decadal variations of ENSO, the Pacific decadal oscillation and tropical cyclones in the western North Pacific. Prog Oceanogr 105:67–80

Li Z, Yu W, Li T, Murty VSN, Tangang F (2013) Bimodal character of cyclone climatology in the Bay of Bengal modulated by monsoon seasonal cycle. J Clim 26:1033–1046

Liu KS, Chan JCL (2008) Interdecadal variability of western North Pacific tropical cyclone tracks. J Clim 21:4464–4476

Liu KS, Chan JCL (2013) Inactive period of western North Pacific tropical cyclone activity in 1998–2011. J Clim 26:2614–2630

Lupo AR, Johnston GJ (2000) The variability in Atlantic Ocean Basin hurricane occurrence and intensity as related to ENSO and the North Pacific Oscillation. Nat Wea Dig 24(1–2):3–13

Lupo AR, Latham TK, Magill TH (2008) The interannual variability of hurricane activity in the Atlantic and East Pacific regions. Natl Weather Dig 32:11–33

Mann HB (1945) Non-parametric test against trend. Econometrica 13:245–259. doi:10.2307/1907187

Mann HB, Whitney DR (1947) On a test of whether one of two random variables is stochastically larger than the other. Ann Math Stat 18:50–60. doi:10.1214/aoms/1177730491

Mantua NJ, Hare SR, Zhang Y, Wallace JM, Francis RC (1997) A Pacific decadal climate oscillation with impacts on salmon. Bull Am Meteorol Soc 78:1069–1079

Mantuna NJ, Hare SR (2002) The Pacific decadal oscillation. J Oceanogr 58:35–44

Matsuura T, Yumoto M, Iizuka S (2003) A mechanism of interdecadal variability of tropical cyclone activity over the western North Pacific. Clim Dyn 21:105–117

Maue RN (2011) Recent historically low global tropical cyclone activity. Geophys Res Lett 38:L14803. doi:10.1029/2011GL047711

McPhaden MJ (2002) El Niño and La Niña: causes and global consequences. In: Munn T (ed) Encyclopedia of global environmental change. Wiley, Chichester, pp 353–370

Power SB, Casey T, Folland C, Colman A, Mehta V (1999) Interdecadal modulation of the impact of ENSO on Australia. Clim Dyn 15:319–324

Ren F, Liang J, Wu G, Dong W, Yang X (2011) Reliability analysis of climate change of tropical cyclone activity over the western North Pacific. J Clim 24:5887–5898

Shen CW, Wang W-C, Gong W, Hao Z (2006) A Pacific decadal oscillation record since 1470 AD reconstructed from proxy data of summer rainfall over eastern China. Geophys Res Lett 33:L03702. doi:10.1029/2005GL024804

Simiu E, Scanlon RH (1978) Wind effects on structures. Wiley Interscience, London, p 458

Smith T, Reynolds R, Peterson T, Lawrimore J (2008) Improvements to NOAA's historical merged land-ocean surface temperature analysis (1880–2006). J Clim 21:2283–2296

Song J-J, Wang Y, Wu L (2010) Trend discrepancies among three best track data sets of western North Pacific tropical cyclones. J Geophys Res 115:D12128. doi:10.1029/2009JD013058

Tao L, Wu L, Wang Y, Yang L (2012) Influence of tropical Indian Ocean warming and ENSO on tropical cyclone activity over the western North Pacific. J Meteorol Soc Jpn 90:127–144

Tu JY, Chou C, Chu PS (2009) The abrupt shift of typhoon activity in the vicinity of Taiwan and its association with western North Pacific-East Asian climate change. J Clim 22(13):3617–3628

Wang B, Chan JCL (2002) How strong ENSO events affect tropical storm activity over the western North Pacific. J Clim 13:1517–1536

Wang C, Picaut J (2004) Understanding ENSO physics—a review. In: Wang C, Xie S-P, Carton JA (eds) Earth's climate: the ocean–atmosphere interaction. Geophysical Monograph Series, vol 147. AGU, Washington, DC, pp 21–48

Wang B, Zhou X (2008) Climate variability and predictability of rapid intensification in tropical cyclones in the western North Pacific. Meteorol Atmos Phys. doi:10.1007/s00703-006-0238-z

Wang C, Weisberg RH, Virmani J (1999) Western Pacific interannual variability associated with the El Niño-Southern oscillation. J Geophys Res 104:5131–5149

Wang B, Wu R, Fu X (2000) Pacific-East Asian teleconnection: how does ENSO affect Asian climate? J Clim 13:1517–1536

Wang L, Chen W, Huang R (2008) Interdecadal modulation of PDO on the impact of ENSO on the east Asian winter monsoon. Geophys Res Lett 35:L20702. doi:10.1029/2008GL035287

Wang X, Wang DX, Zhou W (2009a) Decadal variability of twentieth-century El Niño and La Nia occurrence from observations and IPCC AR4 coupled models. Geophys Res Lett. doi:10.1019/200GL3929

Wang Y, Li S, Luo D (2009b) Seasonal response of Asian monsoonal climate to the Atlantic multidecadal oscillation. J Geophys Res 114:D02112. doi:10.1029/2008JD010929

Wang B, Yang Y, Ding Q, Murakami H, Huang F (2010) Climate control of the global tropical storm days (1965–2008). Geophys Res Lett 37:L07704. doi:10.1029/2010GL042487

Wang C, Li C, Mu M, Duan W (2013) Seasonal modulations of different impacts of two types of ENSO events on tropical cyclone activity in the western North Pacific. Clim Dyn 40:2887–2902

Wang XD, Wang C, Zhang L, Wang X (2015) Multidecadal variability of tropical cyclone rapid intensificatin in the western North Pacific. J Clim 28:3806–3820

Weisberg RH, Wang C (1997) A western Pacific oscillator paradigm for the El Niño-Southern oscillation. Geophys Res Lett 24(7):779–782

Wilcoxon F (1945) Individual comparisons by ranking methods. Biom Bull 1:80–83. doi:10.2307/3001968

Wu L, Wang B (2008) What has changed the proposition of intense hurricanes in the last 30 years? J Clim 21:1432–1439

Wu L, Zhao H (2012) Dynamically derived tropical cyclone intensity changes over the western North Pacific. J Clim 25:89–98

Xiang B, Wang B, Li T (2013) A new paradigm for the predominance of standing Central Pacific warming after the late 1990s. Clim Dyn. doi:10.1007/s00382-012-1427-8

Xie SP, Hu KM, Hafner J, Tokinaga H, Du Y, Huang G, Sampe T (2009) Indian Ocean capacitor effect on Indo-western Pacific climate during the summer following El Niño. J Clim 22:730–747

Yokoi S, Takayabu YN (2013) Attribution of decadal variability in tropical cyclone passage frequency over the western North Pacific: a new approach emphasizing the genesis location of cyclones. J Clim 26:973–987

Yumoto M, Matsuura T (2001) Interdecadal variability of tropical cyclone activity in the western North Pacific. J Meteorol Soc Jpn 79:23–35

Zhan R, Wang Y, Lei X (2011) Contributions of ENSO and east Indian Ocean SSTA to the interannual variability of Northwest Pacific tropical cyclone frequency. J Clim 24:509–521

Zhang Y, Wallace J-M, Battisti D-S (1997) ENSO-like interdecadal variability: 1900–93. J Clim 10:1004–1020

Zhang R-H, Busalacchi A-J, Xue Y (2007) Decadal change in the relationship between the oceanic entrainment temperature and thermocline depth in the far western tropical Pacific. Geophys Res Lett 34:L23612. doi:10.1029/2007GL032119

Zhang Q, Liu Q, Wu L (2009) Tropical cyclone damages in China 1983–2006. Bull Am Meteorol Soc 90:489–495

Zhang L, Wang C, Song Z, Lee S-K (2014) Remote effect of the model cold bias in the tropical North Atlantic on the warm bias in the tropical southeastern Pacific. J Adv Model Earth Syst 6:1016–1026

Zhao H, Wu L, Zhou W (2010) Assessing the influence of the ENSO on tropical cyclone prevailing tracks in the western North Pacific. Adv Atmos Sci 27(6):1361–1371

Zhao H, Wu L, Zhou W (2011) Interannual changes of tropical cyclone intensity in the western north Pacific. J Meteorol Soc Jpn 89(3):243–253. doi:10.2151/jmsj.2011-305

Zhao H, Wu L, Wang R (2014a) Decadal variations of intense tropical cyclones over the Western North Pacific during 1948–2010. Adv Atmos Sci 31(1):57–65. doi:10.1007/s00376-013-3011-5

Zhao H, Chu P-S, Hsu P-C, Muarkami H (2014b) Exploratory analysis of extremely low tropical cyclone activity during the late season of 2010 and 1998 over the western North Pacific and the South China Sea. J Adv Model Earth Syst. doi:10.1002/2014MS000381